

$$I_1 = \frac{1}{\Gamma(m_D)\Gamma(m_{s_D})\Gamma(m_E)\Gamma(m_{s_E})} \left(\frac{\Xi_E}{\Xi_D}\right)^{m_E} G_{1,1:2,2:2,2}^{1,1:1,2:1,2} \left(\begin{matrix} 1-m_D-m_E & 1,1 \\ m_{s_D}-m_E & 1,0 \end{matrix} \middle| \begin{matrix} 1-m_E+m_{s_E}, 1-m_E \\ 0, -m_E \end{matrix} \middle| \frac{1}{\Xi_D}, \frac{\Xi_E}{\Xi_D} \right) \quad (6)$$

$$I_2 = \frac{1}{\Gamma(m_E)\Gamma(m_{s_E})\Gamma(m_D)\Gamma(m_{s_D})} \left(\frac{\Xi_D}{\Xi_E}\right)^{m_D} G_{1,1:2,2:2,2}^{1,1:1,2:1,2} \left(\begin{matrix} 1-m_E-m_D & 1,1 \\ m_{s_E}-m_D & 1,0 \end{matrix} \middle| \begin{matrix} 1-m_D+m_{s_D}, 1-m_D \\ 0, -m_D \end{matrix} \middle| \frac{1}{\Xi_E}, \frac{\Xi_D}{\Xi_E} \right) \quad (7)$$

$$\text{SOP} = \frac{\Xi_D^{m_D}}{\Gamma(1-m_E)\Gamma(m_D)\Gamma(m_{s_D})\Gamma(m_E)\Gamma(m_{s_E})(1-\theta)} \left(\frac{\theta}{\Xi_E}\right)^{1+m_D} \left(1 + \frac{\theta}{(1-\theta)\Xi_E}\right)^{-m_E} \left(1 + \frac{1-\theta}{\theta}\Xi_E\right)^{1+m_D-m_{s_E}} \\ \times G_{1,1:1,1:2,2}^{1,1:1,1:1,2} \left(\begin{matrix} -m_D & m_E \\ m_{s_E}+m_E-m_D-1 & 0 \end{matrix} \middle| \begin{matrix} 1-m_D+m_{s_D}, 1-m_D \\ 0, -m_D \end{matrix} \middle| 1 + \frac{\theta}{(1-\theta)\Xi_E}, \Xi_D(1-\theta) \left(1 + \frac{\theta}{(1-\theta)\Xi_E}\right) \right) \quad (13)$$

$$I_3 = \int_0^\infty \ln(1+\gamma_E) f_E(\gamma_E) d\gamma_E. \quad (5)$$

Accordingly, I_1 and I_2 over Fisher-Snedecor \mathcal{F} fading scenarios are given in (6) and (7) at the top of this page. In addition, I_3 is expressed as

$$I_3 = \frac{1}{\Gamma(m_E)\Gamma(m_{s_E})} G_{3,3}^{2,3} \left(\begin{matrix} 1-m_E, 1, 1 \\ m_{s_E}, 1, 0 \end{matrix} \middle| \frac{1}{\Xi_E} \right) \quad (8)$$

where $G_{c,d}^{a,b}(\cdot)$ and $G_{c_1,d_1:\dots:c_n,d_n}^{a_1,b_1:\dots:a_n,b_n}(\cdot)$ are Meijer G-function and EGBMGF, respectively.

Proof: Substituting (1) and (2) in (3), we have

$$I_1 = \frac{\Xi_D^{m_D} \Xi_E^{m_E}}{m_E B(m_D, m_{s_D}) B(m_E, m_{s_E})} \\ \times \int_0^\infty \ln(1+\gamma_D) \gamma_D^{m_D+m_E-1} (1+\Xi_D\gamma_D)^{-(m_D+m_{s_D})} \\ \times {}_2F_1(m_E+m_{s_E}, m_E; m_E+1; -\Xi_E\gamma_D) d\gamma_D \quad (9)$$

Invoking the identities [8, (11)], [8, (10)], and [8, (17)] with some mathematical manipulations, (9) can be rewritten as

$$I_1 = \frac{\Xi_D^{m_D} \Xi_E^{m_E}}{\Gamma(m_D)\Gamma(m_{s_D})\Gamma(m_E)\Gamma(m_{s_E})} \\ \times \int_0^\infty \gamma_D^{m_D+m_E-1} G_{2,2}^{1,2} \left(\begin{matrix} 1, 1 \\ 1, 0 \end{matrix} \middle| \gamma_D \right) \\ \times G_{1,1}^{1,1} \left(\begin{matrix} 1-m_D-m_{s_D} \\ 0 \end{matrix} \middle| \Xi_D\gamma_D \right) \\ \times G_{2,2}^{1,2} \left(\begin{matrix} 1-m_E-m_{s_E}, 1-m_E \\ 0, -m_E \end{matrix} \middle| \Xi_E\gamma_D \right) d\gamma_D \quad (10)$$

Using [9, (9)] to compute the integral in (10) and doing some mathematical simplifications, (6) is yielded which completes the proof of I_1 .

Following the same steps that are employed to derive I_1 , I_2 can be deduced in closed-form expression as given in (7).

To obtain I_3 , we substitute (1) in (5) and recall the identity

[8, (11)]. Thus, this yields

$$I_3 = \frac{\Xi_E^{m_E}}{B(m_E, m_{s_E})} \\ \times \int_0^\infty \gamma_E^{m_E-1} (1+\Xi_E\gamma_E)^{-(m_E+m_{s_E})} G_{2,2}^{1,2} \left(\begin{matrix} 1, 1 \\ 1, 0 \end{matrix} \middle| \gamma_E \right) d\gamma_E \quad (11)$$

Employing [10, (2.24.2.4)], (8) is yielded which completes the proof of I_3 . ■

IV. SECURE OUTAGE PROBABILITY

The SOP can be evaluated by [2, (14)]

$$\text{SOP} = \int_0^\infty F_D(\theta\gamma_E + \theta - 1) f_E(\gamma_E) d\gamma_E \quad (12)$$

where $\theta = \exp(R_s) \geq 1$ with $R_s \geq 0$ is the target secrecy threshold.

The SOP can be expressed in exact closed-form as given in (13) at the top of this page.

Proof: Inserting (1) and (2) in (12), the result is

$$\text{SOP} = \frac{\Xi_D^{m_D} \Xi_E^{m_E}}{m_D B(m_D, m_{s_D}) B(m_E, m_{s_E})} \\ \times \int_0^\infty \gamma_E^{m_E-1} (\theta\gamma_E + \theta - 1)^{m_D} (1+\Xi_E\gamma_E)^{-(m_E+m_{s_E})} \\ \times {}_2F_1(m_D+m_{s_D}, m_D; m_D+1; \\ -\Xi_D(\theta\gamma_E + \theta - 1)) d\gamma_E \quad (14)$$

Assuming $x = \theta\gamma_E + \theta - 1$ and $dx = \theta d\gamma_E$ and performing some mathematical simplifications, (14) becomes as follows

$$\text{SOP} = \frac{\Xi_D^{m_D}}{m_D B(m_D, m_{s_D}) B(m_E, m_{s_E}) (1-\theta)} \\ \times \left(1 + \frac{\theta}{(1-\theta)\Xi_E}\right)^{-m_E} \left(1 + \frac{1-\theta}{\theta}\Xi_E\right)^{-m_{s_E}} \\ \times \int_0^\infty x^{m_D} \left(1 + \frac{1}{1-\theta}x\right)^{m_E-1} \\ \times \left(1 + \frac{\Xi_E}{\theta + (1-\theta)\Xi_E}x\right)^{-(m_E+m_{s_E})} \\ \times {}_2F_1(m_D+m_{s_D}, m_D; m_D+1; -\Xi_D x) dx \quad (15)$$

$$\text{SOP}^L = \frac{1}{\Gamma(m_E)\Gamma(m_{s_E})\Gamma(m_D)\Gamma(m_{s_D})} \left(\frac{\theta \Xi_D}{\Xi_E} \right)^{m_D} G_{3,3}^{2,3} \left(\begin{matrix} 1 - m_E - m_D, 1 - m_D - m_{s_D}, 1 - m_D \\ m_{s_E} - m_D, 0, -m_D \end{matrix} \middle| \frac{\theta \Xi_D}{\Xi_E} \right) \quad (18)$$

Utilising the identities [8, (10)] and [8, (17)], (15) is expressed as

$$\begin{aligned} \text{SOP} &= \frac{\Xi_D^{m_D}}{\Gamma(1 - m_E)\Gamma(m_D)\Gamma(m_{s_D})\Gamma(m_E)\Gamma(m_{s_E})(1 - \theta)} \\ &\times \left(1 + \frac{\theta}{(1 - \theta)\Xi_E} \right)^{-m_E} \left(1 + \frac{1 - \theta}{\theta}\Xi_E \right)^{-m_{s_E}} \\ &\times \int_0^\infty x^{m_D} G_{1,1}^{1,1} \left(\begin{matrix} m_E \\ 0 \end{matrix} \middle| \frac{1}{1 - \theta} x \right) \\ &\times G_{1,1}^{1,1} \left(\begin{matrix} 1 - m_E - m_{s_E} \\ 0 \end{matrix} \middle| \frac{\Xi_E}{\theta + (1 - \theta)\Xi_E} x \right) \\ &\times G_{2,2}^{1,2} \left(\begin{matrix} 1 - m_D - m_{s_D}, 1 - m_D \\ 0, -m_D \end{matrix} \middle| \Xi_D x \right) dx \quad (16) \end{aligned}$$

Making use of [9, (9)], the derived result in (13) is yielded

V. LOWER BOUND OF THE SECURE OUTAGE PROBABILITY

The SOP^L can be computed by [2, (17)]

$$\text{SOP}^L = \int_0^\infty F_D(\theta\gamma_E) f_E(\gamma_E) d\gamma_E \quad (17)$$

The SOP^L over Fisher-Snedecor \mathcal{F} fading scenarios can be derived as given in (18) at the top of this page.

Proof: Plugging (1) and (2) in (17) and doing some mathematical manipulations, we have

$$\begin{aligned} \text{SOP}^L &= \frac{\theta^{m_D} \Xi_D^{m_D}}{B(m_E, m_{s_E})\Gamma(m_D)\Gamma(m_{s_D})\Xi_E^{m_{s_E}}} \\ &\times \int_0^\infty \gamma_E^{m_E + m_D - 1} \left(\frac{1}{\Xi_E} + \gamma_E \right)^{-(m_E + m_{s_E})} \\ &\times {}_2F_1(m_D + m_{s_D}, m_D; m_D + 1; -\theta\Xi_D x) d\gamma_E \quad (19) \end{aligned}$$

With the help of [8, (17)], (19) can be rewritten as

$$\begin{aligned} \text{SOP}^L &= \frac{\theta^{m_D} \Xi_D^{m_D}}{B(m_E, m_{s_E})\Gamma(m_D)\Gamma(m_{s_D})\Xi_E^{m_{s_E}}} \\ &\times \int_0^\infty \gamma_E^{m_E + m_D - 1} \left(\frac{1}{\Xi_E} + \gamma_E \right)^{-(m_E + m_{s_E})} \\ &\times G_{2,2}^{1,2} \left(\begin{matrix} 1 - m_D - m_{s_D}, 1 - m_D \\ 0, -m_D \end{matrix} \middle| \Xi_D \theta \gamma_E \right) d\gamma_E \quad (20) \end{aligned}$$

Utilising [10, (2.23.2.4)] to compute the integral in (20), the result in (18) is deduced and this completes the proof. ■

VI. STRICTLY POSITIVE SECURE CAPACITY

The SPSC is expressed as [2, (20)]

$$\text{SPSC} = 1 - \text{SOP} \quad \text{for } \theta = 1 \quad (21)$$

Consequently, the SPSC over Fisher-Snedecor \mathcal{F} fading channels can be obtained by using (13) and $\theta = 1$ and inserting the result in (21).

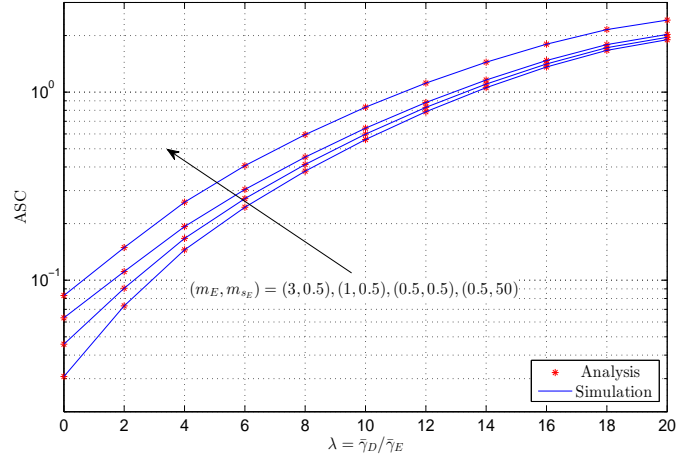


Fig. 1. ASC over Fisher-Snedecor \mathcal{F} fading channels versus λ for different values of (m_E, m_{s_E}) , $\bar{\gamma}_E = 5$ dB, $m_D = 2.5$, and $m_{s_D} = 5$.

VII. ANALYTICAL AND SIMULATION RESULTS

In this section, to validate our derived expressions of the physical layer security over Fisher-Snedecor \mathcal{F} fading channels, the Monte Carlo simulations that are obtained via generating 10^7 realizations are compared with the analytical results. In all figures, the simulations and the numerical results of the performance metrics that are plotted versus $\lambda = \bar{\gamma}_D / \bar{\gamma}_E$ for $m_D = 2.5$ and $m_{s_D} = 5$ (moderate shadowing) are represented by the solid lines and the stars, respectively. Moreover, two different scenarios of the shadowing impact at the eavesdropper which are light and heavy shadowing are studied by using $m_{s_E} = 0.5$ and $m_{s_E} = 50$, respectively. In all results, a MATHEMATICA code that is provided in [9] has been used to calculate the EGBMGF. This is because it is not available as a built in function in MATLAB and MATHEMATICA software packages.

Figs. 1-5 show the ASC, the SOP, the SOP^L , and the SPSC over Fisher-Snedecor \mathcal{F} fading channels for $\bar{\gamma}_E = 5$ dB and different values of the fading parameters m_E and m_{s_E} . In these figures, it can be observed that the performance becomes better, when m_{s_E} increases. This is because small and large values of m_{s_E} correspond to light and heavy shadowing, respectively. For instance, in Fig. 1, when $\lambda = 6$ and $m_E = 0.5$ (fixed), the ASC for $m_{s_E} = 50$ is approximately 25% higher than $m_{s_E} = 0.5$. In the same context, when m_E increases, the ASC decreases. This refers to less impact of the multipath on the Eve which would lead to reduce the total ASC.

In Figs. 2 and 4 that are plotted for $R_s = 1$ bit/s/Hz, one can see that the values of SOP are greater than or equal to the SOP^L which confirms our derived expressions. Furthermore, another confirmation that proves the validation of our analysis is the perfect matching between the numerical results and their Monte Carlo simulation counterparts in all provided figures.

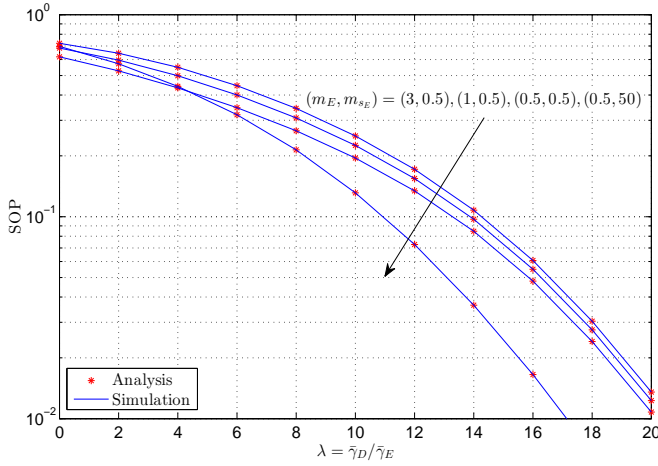


Fig. 2. SOP over Fisher-Snedecor \mathcal{F} fading channels versus λ for different values of (m_E, m_{s_E}) , $\bar{\gamma}_E = 5$ dB, $m_D = 2.5$, $m_{s_D} = 5$, and $R_s = 1$.

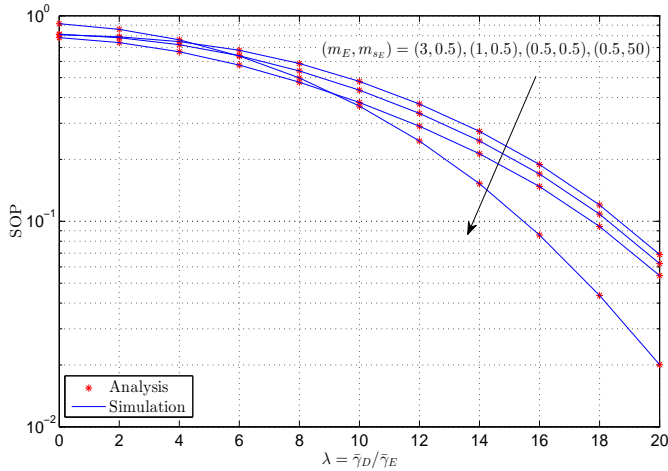


Fig. 3. SOP over Fisher-Snedecor \mathcal{F} fading channels versus λ for different values of (m_E, m_{s_E}) , $\bar{\gamma}_E = 5$ dB, $m_D = 2.5$, $m_{s_D} = 5$, and $R_s = 2$.

VIII. CONCLUSIONS

In this letter, the secrecy performance of physical layer over Fisher-Snedecor \mathcal{F} fading channels is analysed. Specifically, the ASC, the SOP, the SOP^L , and the SPSC are derived in exact mathematically tractable closed-form expressions. The results of this work provide a good insight about the security of the physical layer over composite multipath/shadowing fading channels when the wireless channels subject to heavy, moderate, or light shadowing. Moreover, the analysis of the physical layer security over different scenarios can be deduced from the derived expressions by setting m and m_s for specific values such as the Nakagami- m fading condition is obtained by inserting $m_s \rightarrow \infty$ and $m = \mathbf{m}$ where \mathbf{m} is the Nakagami- m multipath index.

REFERENCES

- [1] A. D. Wyner, "The wire-tap channel," *Bell Syst. Tech. J.*, vol. 54, no. 8, pp. 1355-1387, Oct. 1975.
- [2] H. Al-Hmood, and H. Al-Rawashidy, "Secrecy analysis of physical layer over $\kappa - \mu$ shadowed fading scenarios," *IEEE Access*, Submitted April 2018, <https://arxiv.org/abs/1804.09208>.

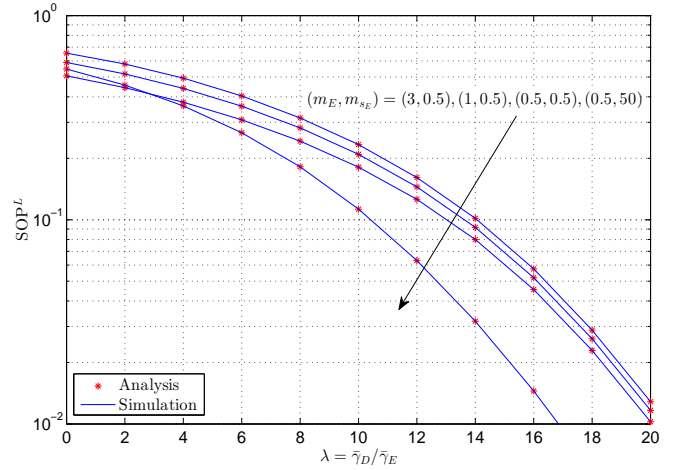


Fig. 4. SOP^L over Fisher-Snedecor \mathcal{F} fading channels versus λ for different values of (m_E, m_{s_E}) , $\bar{\gamma}_E = 5$ dB, $m_D = 2.5$, $m_{s_D} = 5$, and $R_s = 1$.

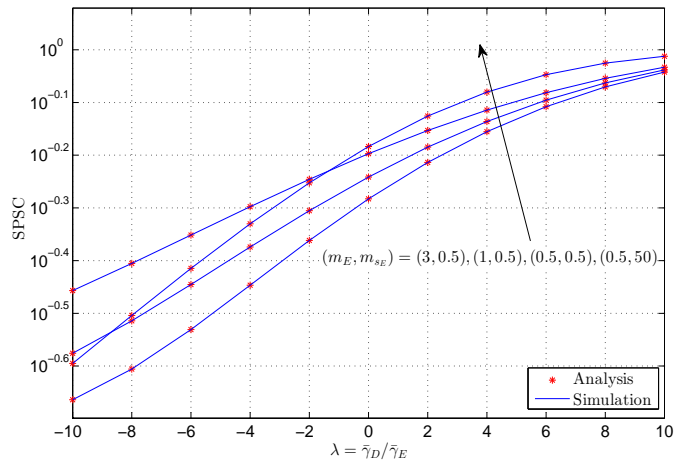


Fig. 5. SPSC over Fisher-Snedecor \mathcal{F} fading channels versus λ for different values of (m_E, m_{s_E}) , $\bar{\gamma}_E = 5$ dB, $m_D = 2.5$, and $m_{s_D} = 5$.

- [3] H. Lei, H. Zhang, I. S. Ansari, C. Gao., Y. Guo, G. Pan, and K. A. Qaraqe, "Physical layer security over generalized- K fading channels," *IET Commun.*, vol. 10, no. 16, pp. 2233-2237, July 2016.
- [4] H. Lei, H. Zhang, I. S. Ansari, C. Gao., Y. Guo, G. Pan, and K. A. Qaraqe, "Performance analysis of physical layer security over generalized- K fading channels using a mixture gamma distribution," *IEEE Commun. Lett.*, vol. 20, no. 2, pp. 408-411, Feb. 2016.
- [5] S. K. Yoo, S. L. Cotton, P. C. Sofotasios, M. Matthaiou, M. Valkama, and G. K. Karagiannidis, "The Fisher-Snedecor \mathcal{F} distribution: A simple and accurate composite fading model" *IEEE Commun. Lett.*, vol. 21, no. 7, pp. 1661-1664, March 2017.
- [6] H. Al-Hmood, "Performance of cognitive radio systems over $\kappa - \mu$ shadowed with integer μ and Fisher-Snedecor \mathcal{F} fading channels," in *Proc. IEEE IICETA*, Najaf, Iraq, May 2018, To be appear.
- [7] I. S. Gradshteyn, and I. M. Ryzhik, *Table of Integrals, Series and Products*, 7th edition. Academic Press Inc., 2007.
- [8] V. S. Adamchik and O. I. Marichev, "The algorithm for calculating integrals of hypergeometric type functions and its realization in REDUCE system," in *Proc. IEEE ISSAC*, Tokyo, Japan, Aug. 1990, pp. 212-224.
- [9] C. Garcia-Corrales, F. J. Cañete, and J. F. Paris, "Capacity of $\kappa - \mu$ shadowed fading channels," *Int. J. of Antennas and Propagation*, vol. 2014, pp. 1-8, July 2014.
- [10] A. P. Prudnikov, Yu. A. Brychkov, and O. I. Marichev, *Integrals and Series: More Special Functions*, vol. 3. Gordon and Breach Science Publishers, 1990.